Lateral cyclic loading tests of a full-scale GRS integral bridge model

Masayuki Koda[1], Takahiro Nonaka[2], Motoaki Suga[3], Ryosuke Kuriyama[3], Masaru Tateyama[4] & Fumio Tatsuoka[5]

ABSTRACT

Integral bridges integrate a girder to a pair of abutments without using bearings to resolve several problems due to their use. A great number of bridges of this type have been constructed in the UK and the North America. However, as the backfill is not reinforced, several other problems take place by seasonal thermal contraction and expansion of the girder and seismic loading. To alleviate these problems, a new type of bridge, called Geosynthetic-Reinforced Soil (GRS) integral bridge, has been developed, which integrates a girder, a pair of abutments (i.e., full-height rigid facings) and the backfill reinforced with geosynthetic reinforcement connected to the back of the facings. To validate high performance of GRS integral bridge when subjected to thermal effects and severe seismic loads, a series of lateral cyclic loading tests were performed on a full-scale model comprising a 14.75 m-long girder and 5.55 m-high facings with a width of 3 m. Large loads simulating very high seismic loads (so-called Level 2) were applied. The GRS integral bridge model performed very well when subjected to these two types of cyclic loading.

INTRODUCTION

A conventional type bridge typically has a girder that is simple-supported by a pair of abutments via a pair of bearings (i.e., a fixed/pin and a movable/roller). The approach fills are not reinforced and constructed retained by the abutments that have been constructed in advance. For these structural features and construction sequence, several problems often take place. Firstly, as the abutments are a

[1-4] Masayuki Koda, Takahiro Nonaka, Motoaki Suga, Ryosuke Kuriyama and Masaru Tateyama: Railway Technical Research Institute, 2-8-38 Hikari-cho, Kokubunji, Tokyo, 185-8540, Japan
[5] Fumio Tatsuoka: Tokyo University of Science, 2641 Yamazaki, Noda, Chiba, 278-8510, Japan

cantilever structure, with an increase in the abutment height and with a decrease in the bearing capacity of the supporting ground, the cost for the abutments supported by piles becomes increasing higher to keep small the displacements of the abutments caused by earth pressure and ground movements associated with the construction of approach fills. Secondly, the cost for: 1) installation of bearings with arrangements to prevent the dislodging of the girder by seismic loads; and 2) long-term maintenance to prevent the corrosion of the bearings is very high. Thirdly, the seismic stability of the cantilever-type abutments and unreinforced backfill is rather low. Fourthly, a relatively large bumping may develop immediately back of the abutment gradually by self-weight and long-term traffic loads and suddenly by seismic loads enhanced by displacements of the abutment and deformation of the supporting ground.

To alleviate the problems due to the use of bearings with the conventional type bridges, integral bridges were developed and many have been constructed in the UK and the North America. This type of bridge comprises a continuous girder that is structurally integrated to a pair of abutments without using bearings. However, as the backfill is unreinforced and constructed after the abutments have been constructed, many problems of the conventional type bridges remains unsolved. Besides, a new problem develops. That is, the backfill is cyclically displaced in the lateral direction by thermal deformation of the girder, which results in both residual settlement of the backfill by active failure and development of high passive earth pressure (i.e., the dual ratcheting phenomenon [1, 2].

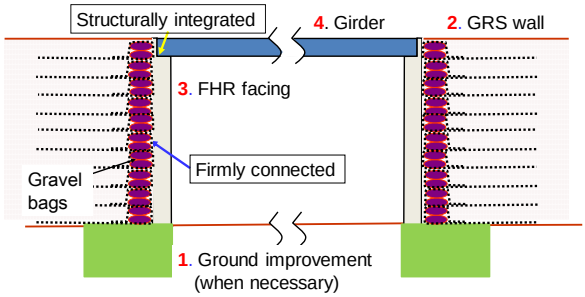

Figure 1. GRS integral bridge: the numbers show the construction sequence [1]

Results from a series of model tests (i.e., cyclic static loading tests simulating thermal effects and shaking table tests simulating seismic loading) [1, 2] showed that these problems with the integral bridge can be alleviated while maintaining the advantages of the integral bridge by reinforcing the backfill with reinforcement layers connected to the back of the abutments (i.e., the full-height rigid (FHR) facings). This new type bridge is called the Geosynthetic-Reinforced Soil (GRS) integral bridge. As illustrated in Fig. 1, after the deformation of the supporting ground and the backfill associated with the construction of the reinforced backfill has taken place, FHR facings are constructed by casting-in-place concrete on the wall face wrapped-abound with geogrid layers reinforcing the backfill. By this staged-construction procedure and due to the fact that the FHR facings are not a cantilever structure, but they are a continuous beam supported by reinforcement layers at many elevations, the internal forces and the lateral thrust forces and overturning moment at the base become very small compared with the abutments of the conventional type bridge [3, 4]. For this reason, pile foundations are usually not necessary. As the girder and FHR facings constitute a thin RC frame structure, the forces activated in the girder become much lower than those in the

simple-supported girder of the conventional type bridge. Therefore, the girder and facings (i.e., abutments) of GRS integral bridge are much less massive than those of the conventional type bridge under otherwise the same conditions.

A prototype GRS integral bridge was first constructed during a period of 2011 – 2012 for a new high-speed train line in Hokkaido (Hokkaido Shinkansen) [5, this conference]. Three other GRS bridges are now under construction (in the year of 2013) to restore two conventional type bridges and a RC frame structure of Sanriku Railway that totally collapsed by the great tsumani during the 2011 Great East Japan Earthquake [6, 7].

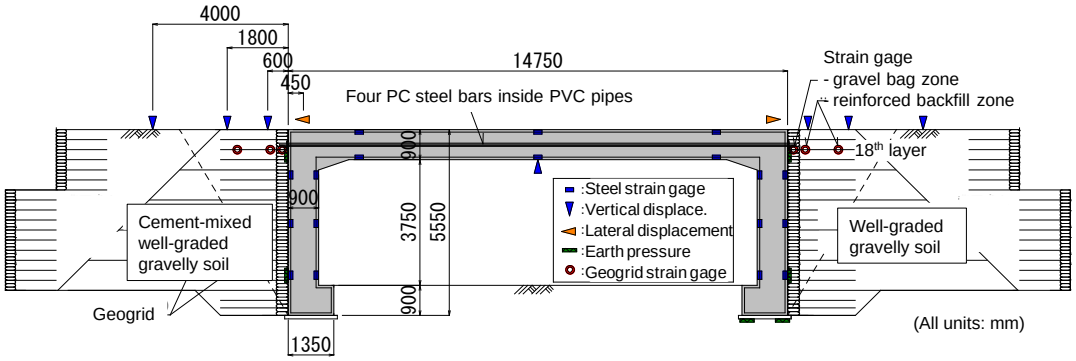

Figure 2. Full-scale model of GRS integral bridge

Figure 3. A general view of the model and arrangements for lateral loading tests

To confirm the details of the actual construction procedure of this new type bridge, a full-scale model of GRS integral bridge was constructed at the Railway Technical Research Institute for a period from the end of 2008 to the beginning of 2009 (Figs. 2 & 3; [8]). The observations of the behavior of the model for two years since the construction showed very small residual deformations in the RC members and the approach blocks made of either cement-mixed gravelly soil or uncemented gravelly soil immediately behind the facings.

The thermal deformation of the girder increases with girder length and with temperature change. In fact, GRS integral bridges having girders longer than 15 m (i.e., the girder length of the full-scale model) are now under construction. The annual temperature changes in other places could be much larger than the one at the place where the full-scale model was constructed (i.e., Tokyo). In view of the above, in the present study, to evaluate effects of the thermal deformation of the girder larger than those that had been observed with the full-scale model, a series of lateral cyclic loading tests using relatively large lateral loads were performed. Besides, to evaluate the performance during such severe seismic loading as experienced during the 1995 Great Kobe Earthquake (so-called Level 2 design seismic load), another series of lateral cyclic loading tests were performed. This paper reports the procedures and results of these cyclic loading tests.

FULL-SCALE GRS INTEGRAL BRIDGE MODEL

The full-scale model of GRS integral bridge (Figs. 2 & 3) is 3.0 m wide simulating a railway bridge for a single-truck line. The model comprises a 14.75 m-long girder, a pair of 5.55 m high FHR facings and a pair of approach blocks.Table1 lists the construction materials and dimensions.

Table 1 Construction materials and dimensions of full-scale GRS integral model

Bridge dimensions	Girder length	14.75 m
	Width	3 m
	Girder thickness	0.9 m
	Facing thickness	0.9 m
	Foundation	Spread footing
Concrete	Cement	Ordianary Portland
	Design compressive strength	f_{ck}= 27 N/mm^2
Steel reinforcement	Type	SD345
	Main reinforcement	D19ctc150mm (Footing & facings)
		D22ctc150mm (Girder)
Geogrid	PVA) fiber covered with PVC Design tensile rupture strength	T_a= 60 kN/m
Approach fill	Well-graded gravelly soil (WG GS)	M-40
	Cement-mixed WG GS	M-40 mixed with ordinary Portland cement
Backfill in back of the approach block		C-40 (crusher run)

Two types of approach block that are currently used for railways in Japan were constructed by compacting either well-grade gravelly soil (GS) (crushed hard rock from a quarry, M-40) or cement-mixed M-40 with a dry weight ratio of cement to gravel equal to 4 %. Well compacted cement-mixed GS is used mainly for high speed train lines to minimize the bumping immediately in back of the abutment. With GRS integral bridges, an increase in the seismic stability of a whole bridge system is another purpose of the use of cement-mixed GS approach block [1]. On the other hand, approach blocks of compacted gravelly soil are used for ordinary train lines. With both approach block types of the full-scale model, the backfill was reinforced with 19 layers of geogrid with a vertical spacing of 30 cm. The geogird

comprises polyvinyl alcohol (PVA) fibre covered with a protection of polyvinyl chloride (PVC). This geogrid type has a very high resistance to high alkaline [9]. This is one of the most important features required for geogrids to be used for GRS integral bridges, as the end part of the geogrid is buried in a concrete layer of the facing for a firm connection.

Figure 4. Wall face of the approach block of cement-mixed gravelly soil under construction (27 November 2008)

Three layers of gravel bags filled with gravelly soil with a compacted thickness of about 10 cm per each and a compacted width of about 40 cm were placed at the shoulder of each soil layer (Fig. 4). With help of these gravel bags, the backfill was compacted so that the compacted soil layer thickness became 15 cm with at least a degree of compaction of 95 % by modified Proctor. The compressive strength of compacted cement-mixed gravel was designed to be at least 2 MPa at a curing day of 28 days. Immediately in back of the facing of both completed approach blocks, there exists a pile of bags filled with gravel with each bag being wrapped-around with a geogrid reinforcing the backfill and firmly connected to the facing. The gravel bag zone functions as a drain during rainfalls and a mechanical protection for the grid/facing connections against strong loading during severe earthquakes. When the approach block of cement-mixed gravel approach block is constructed, it also absorbs cyclic displacements caused by seasonal thermal deformation of the girder.

Table 2 Measurement items and devices

Items	Devices
Tensile force in geogrid reinforcement	Electric-resistance strain gages
Earth pressure on the back of FHR facings	Earth pressure cells
Contact pressure at the bottom face of the footing	Earth pressure cells
Force in steel reinforcement	Electric-resistance strain gages
Displacement of the girder and approach fills	Displacement transducers

OUTLINE OF CYCLIC LOADING TESTS

The measuring devices listed in Table 2 were arranged in the model, as shown in Fig. 2. Tensile forces in the geogrid were measured at six points; lateral earth pressures between the facing and the gravel bag zone at four points (near the top and bottom of each facing); the vertical sub-grade reactions at the bottom face of the footing at two points; stresses in the steel bars at eighteen points, lateral displacements at the upper face of the RC girder (i.e., at the top of the facings) at two points; and settlements at the crests of the two approach blocks at six points.

Table 3 Two series of lateral cyclic loading tests

Loading method	Loading history	Objective
One-side cyclic loading (H: constant single amplitude of lateral load)	50 cycles of H= 500 kN in two directions; and 50 cycles of H= 1,000 kN in two directions	Simulation of seasonal thermal displacements
Reversed cyclic loading with a vertical train load W_{max}= 35 kN/m on the girder (H_{max}: largest lateral load)	H_{max}= 2,300 kN when loading toward cement-mixed GS:	Simulation of Level 2 design seismic load
	H_{max}= 2,600 kN when loading toward gravelly soil	

Table 3 shows the outline of two types of cyclic lateral loading simulating lateral cyclic loads in the bridge axis direction due to 1) thermal expansion and contraction of the girder: and 2) seismic loads up to Level 2 design seismic load. In this loading test program, vertical cyclic loads were also applied to the center of the girder simulating train loads. The results showed that the GRS integral bridge model exhibits very small displacements showing no problem during ordinary long-term service. The vertical loading test will be reported elsewhere.

One-side lateral cyclic loading tests simulating long-term thermal effects

Lateral load was applied to the girder by using four hydraulic jacks with a capacity of 1,000 kN/each on one side (so in total four) fixed to a steel reaction frame arranged at each end of the model (Fig. 2). The tensile load from the jacks was transmitted to four PC steel bars arranged in PVC pipe sheaths buried in the girder via steel rods in sheaths buried in the approach fills on both sides of the model. Both ends of the PC steel bars were fixed to the end faces of the girder using steel plates and bolts so that the loads from the jacks were fully transmitted as compression loads to both ends of the girder.

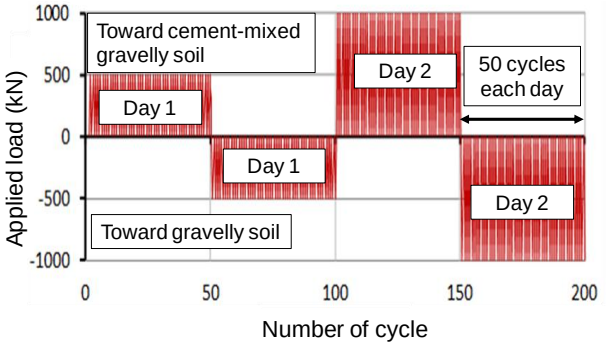

Figure 5. One-side cyclic loading simulating long-term thermal effects

Fig. 5 shows the time histories of cyclic loads applied between zero and the peak load in respective directions: i.e., toward either the approach blocks of gravelly soil (on the right side in Fig. 2) or cement-mixed gravelly soil (on the left side in Fig. 2). No resting time was used between successive cycles. The total test period was two days. The peak load was set equal to 500 kN to simulate an expansion/contraction of the 15 m-long girder due to a change in the temperature equal to 20°C. 50 cycles were applied simulating a period of 50 years. A peak load of 1,000 kN was also applied to examine the behavior by more severe temperature effects.

Reversed lateral cyclic loading tests simulating seismic loading

This study was performed to evaluate the seismic stability of a GRS bridge when subjected to seismic loads in the longitudinal bridge axial direction by applying lateral cyclic loads in the direction of the axis of the GRS integral bridge model. To evaluate the seismic stability when subjected seismic loads in the transversal direction of the bridge axis, another series of cyclic loading tests will be necessary.

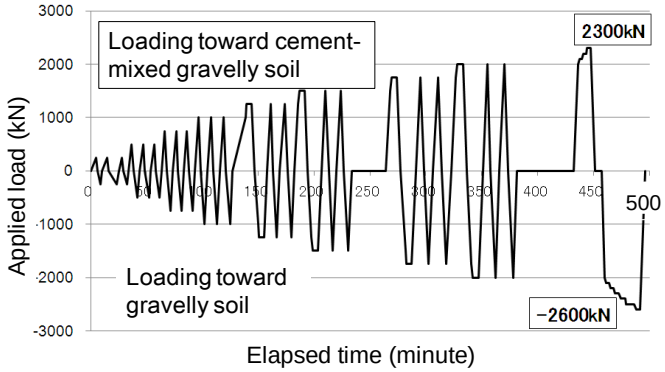

Figure 6. Reversed cyclic loading simulating seismic loading

Fig. 6 shows the time history of reversed cyclic loads applied to evaluate the behavior of the GRS integral model when subjected to seismic loads up to L2 level design seismic load. A series of three symmetric reversed cycles were applied stepwise increasing the single amplitude from 250 kN to 2,000 kN. In the last cycle, a maximum lateral load equal to 2,300kN was applied toward the cement mixed gravelly soil approach block, followed by a maximum load equal to 2,600 kN toward the well-grade gravelly soil approach block. The load was 2,200 kN is equivalent to a peak response acceleration at the girder equal to 1.0 g (i.e., the gravitational acceleration, which is considered of the order of L2 level design seismic load, as discussed in [10].

Unlike these cyclic loading tests, under actual seismic loading conditions, not only the girder but also the facings and the approach fills on both sides are subjected to seismic lateral loads. Therefore, the inertia of the girder is not fully activated as lateral load to the facings and approach fills. So, the effects of lateral loading on the behavior of the approach fills with the FHR facing in these reversed cyclic loading tests are more severe than actual seismic loading for the same inertia of the girder. The same conservative approximation of seismic loading as these

cyclic loading tests is adopted in the current seismic design methodology of GRS integral bridges [10].

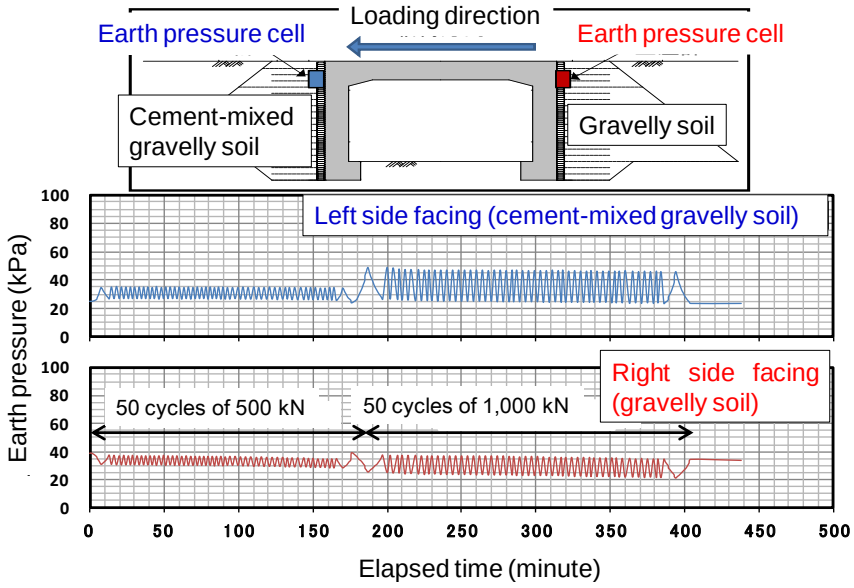

a)

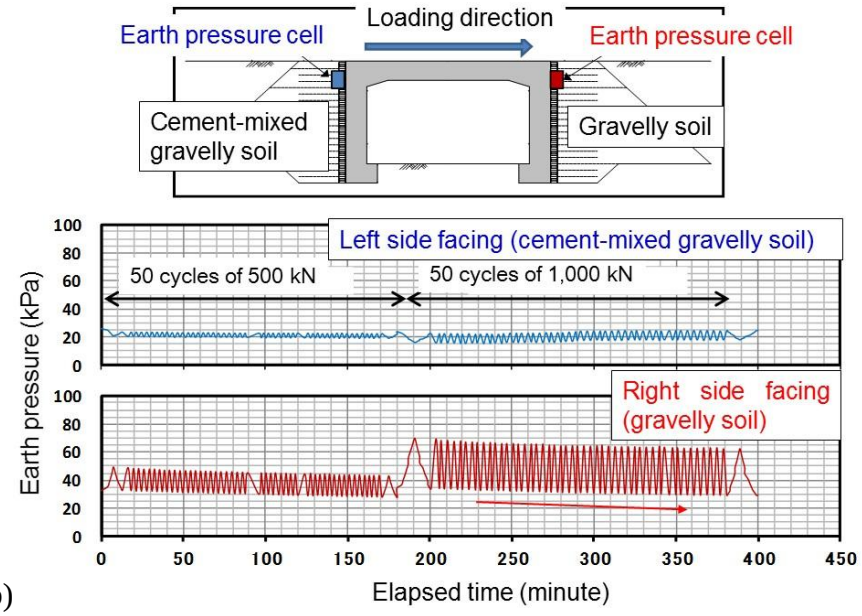

b)

Figure 7. Time histories of earth pressure near the top of the facing by reversed cyclic loads on: a) the cement-mixed gravelly soil side and b) the gravelly soil side

TEST RESULTS

One-side cyclic lateral loading tests simulating thermal loading

Figs. 7a & b show the lateral earth pressures activated near the top of the back of the facing of the respective approach blocks. The earth pressure at both sides decreased and increased according to, respectively, the active and passive displacements of the facing. It may also be seen that the peak earth pressure,

observed in the passive mode, did not increase with cyclic loading, but the value on the gravelly soil approach block side decreased gradually with cyclic loading. This result indicates that a slight pressure redistribution took place along the height of the facing probably associated with gradual yielding in the top part of the gravelly soil approach block. Accordingly, the axial load in the girder did not increase with cyclic loading.

Figs. 8a & b show the relationship between the lateral load and the displacement at the top of the facing on the respective sides. It may be seen that the lateral displacement is of the order of 5 mm irrespective of displacement mode (active or passive) and the backfill type of approach block. This displacement is about 0.1 % of the bridge height (i.e., about 5 m). It may also be seen that the behaviour is highly reversible not indicating developments of residual displacements.

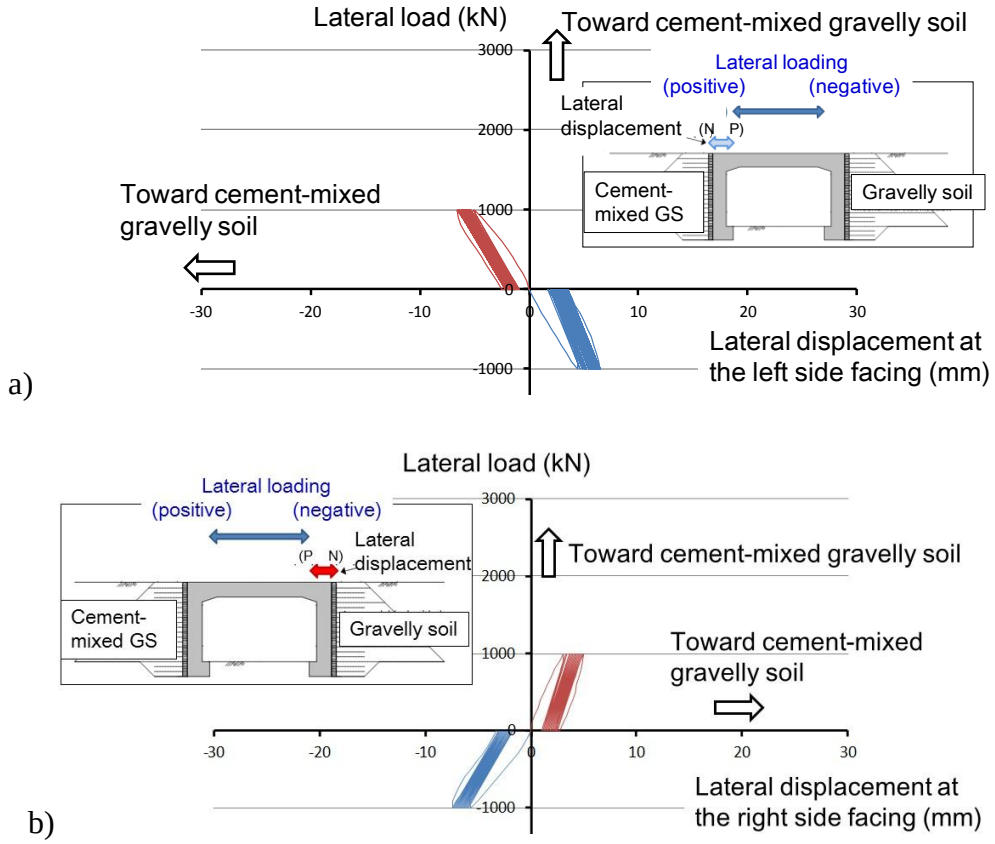

Figure 8. Relationships between the lateral load and the lateral displacement at the top of the facing for: a) cement-mixed gravelly soil approach block; and b) gravelly soil approach fill, for one-side lateral cyclic loads of 1,000 kN.

Fig. 9 shows the settlement on the crest of the approach block at a distance of 60 cm from the back face of the facing (i.e., immediately behind the gravel bag zone) when the load changed between 0 and $\pm$1,000 kN. It may be seen that both cyclic and residual settlements were very small. The maximum residual settlement was of the order of 1 mm, which is far below the allowable limit for railways.

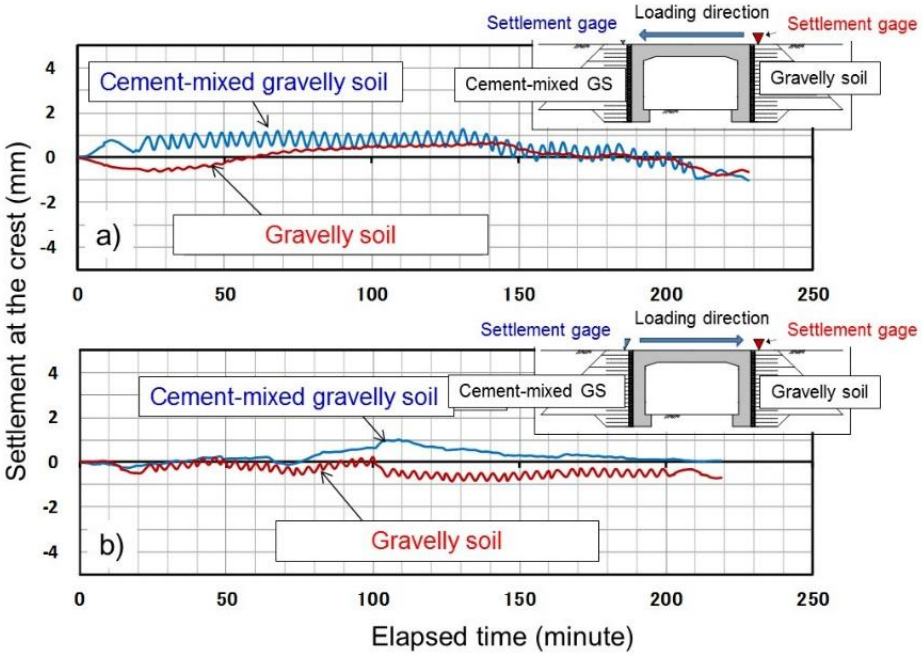

Figure 9. Time histories of settlement at 60 cm in back of the facing of the approach block by one-side cyclic loads with a single load amplitude equal to 1,000 kN on: a) the cement-mixed gravelly soil side; and b)the gravelly soil side

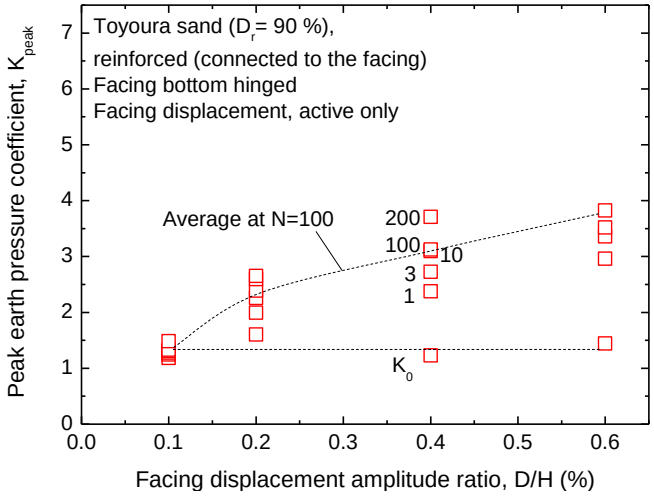

Figure 10. Peak passive earth pressure coefficient when FHR facing is hinged at the bottom for displacements applied only on the active side: the backfill of air-dried Toyoura sand is reinforced with a geogrid connected to the facing [1]

These trends of behaviour of the full-scale model are consistent with the results from lateral cyclic loading tests in the laboratory [1], in which different constant peak lateral displacements were applied at the top of a 50.5 cm-high model facing retaining the backfill of air-dried Toyoura sand reinforced with a model geogrid connected to the back of the facing. As seen from Fig. 10, in those laboratory model tests, when the lateral displacement at the top of the facing ranged from 0.0 % to 0.1 % (active), the earth pressure on the back of the facing did not increase noticeably with the peak earth pressure coefficient K_{peak} being kept to

about 1.5. That is, the behaviour is highly reversible. Moreover, the fact that residual settlement in the full-scale model was very small (Fig. 9) is consistent with the results from the laboratory small scale tests [1] that the settlement at the crest of the backfill behind the facing to which reinforcement layers are connected is kept negligible irrespective of the amplitude of cyclic displacement.

In summary, in the full-scale loading tests, the effects of simulated seasonal thermal deformation of the girder on the stress states and deformation of the girder, facings and approach blocks were negligible. However, the effects should increase with an increase in the length of the girder and the temperature change. The observation of the behavior of two long prototype GRS integral bridges with a girder length of 40 m and 60 m presently under construction for Sanriku Railway [6, 7] will provide information with respect to the effects of girder length.

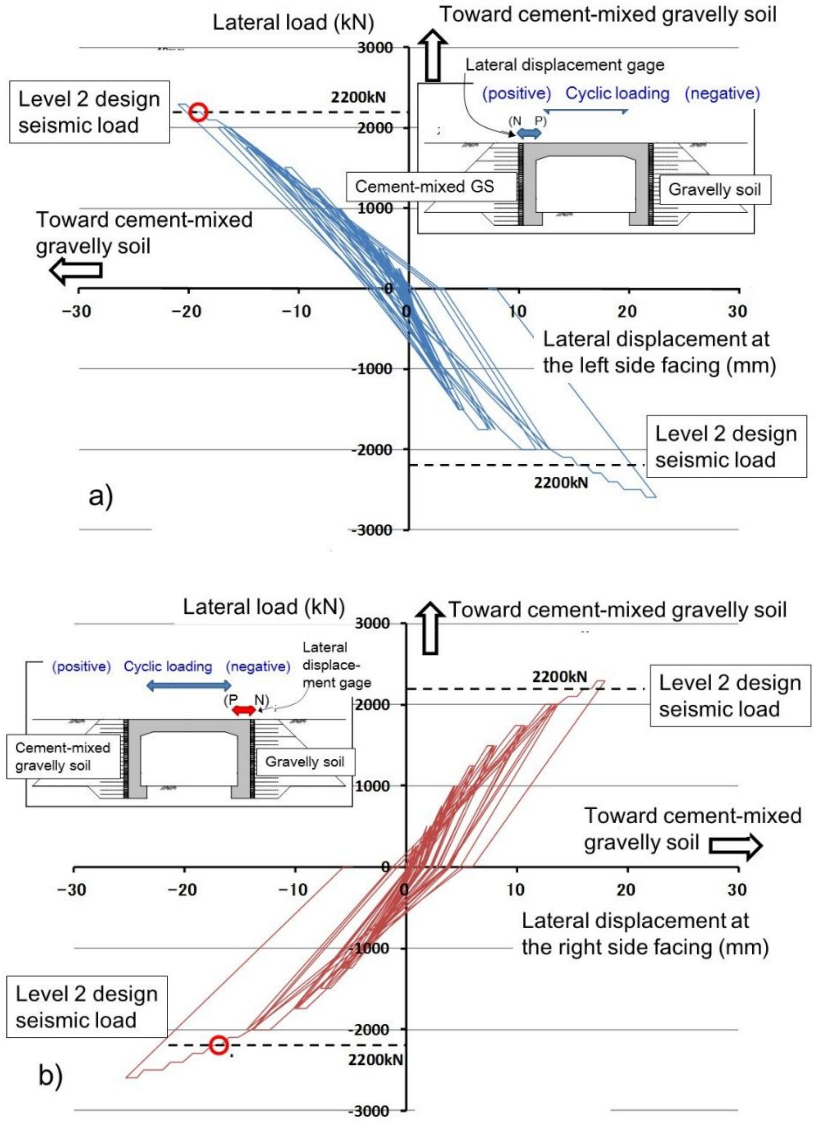

Figure 11. Relationships between the lateral load and the lateral displacement at the top of the facing for: a) cement-mixed gravelly soil approach block; and b) gravelly soil approach fill, from reversed lateral cyclic loading tests.

Reversed lateral cyclic loading tests simulating seismic loading

Figs. 11a & b show the relationships between the lateral load and the lateral displacements at the top of the facing on both sides of the model. Figs. 12a & b show the envelopes of the relationships presented in Figs. 11a & b. It may be seen from these figures that, when the peak lateral load was less than about 1,000 kN, the behavior is highly reversible, showing that the damage to the approach blocks (including the gravel bag zone, the geogrid and the connection between the geogrid and the facing) was very small. This result is consistent with the one from the on-side cyclic loading test simulating thermal effects, presented in the preceding section. As the peak load was increased exceeding about 1,000 kN, the load – displacement relation started exhibiting more noticeable hysteresis curves. In the last cycle, in which the load reached and exceeded the L2 design seismic load, the residual displacements at both sides became particularly large, due probably to yielding of the geogrid at and immediately behind the connection with the facing. Yet, the peak displacements at the facings in the active and passive modes when the tensile load was equal to the L2 seismic load were only about 20 mm on both sides. This very high performance can be attributed to such features of GRS integral bridge as that all the major components (i.e., a girder, a pair of facings and a pair of geosynthetic-reinforced approach blocks) are all integrated to each other and they all together resist applied loads. In particular, unlike the conventional type integral bridge (with unreinforced backfill), the resistance by tensile forces in the geogrid on the active side and that by the compressive loads in the backfill on the passive side are activated simultaneously.

It may also be seen from Fig. 12a that the displacement in the active mode at the top of the facing for the approach block of cement-mixed GS was smaller than that for the approach block of gravelly soil. It may also be seen from Fig. 12b that the displacement in the passive mode at the top of the facing for the approach block of gravelly soil was smaller than that for the approach block of cement-mixed GS. These results show that the displacement of the girder was smaller when the load was activated toward the gravelly soil approach fill (i.e., the cases with a superscript * in Figs. 12a & b) than when the load was activated toward the cement-mixed GS. It is likely that these trends are due to the following two factors:

1) The tensile stiffness of the geogrid in the approach block of cement-mixed GS is larger than that in the approach block of gravelly soil. It is likely that the tensile deformation of the geogrid in the approach block of cement-mixed GS is more restrained due to much higher stiffness of cement-mixed GS.
2) It seems that the coefficient of lateral sub-grade reaction for compression of the approach block of cement-mixed GS is not much larger than that of the approach block of gravelly soil, as the compressive stiffness of the approach block of cement-mixed GS is largely controlled by a much smaller compressive stiffness of the gravel bag zone.

Yet, the differences between the displacements in the active and passive modes at the respective approach fills and between the two types of approach block are not significant. It is likely therefore that the displacements when both approach blocks are made of cement-mixed GS are not largely smaller than that of the stiffer response in Figs. 12a & b, while the displacements at the top of the facing when both approach blocks are made of gravelly soil are not largely larger than that of the softer response presented in Figs. 12a & b.

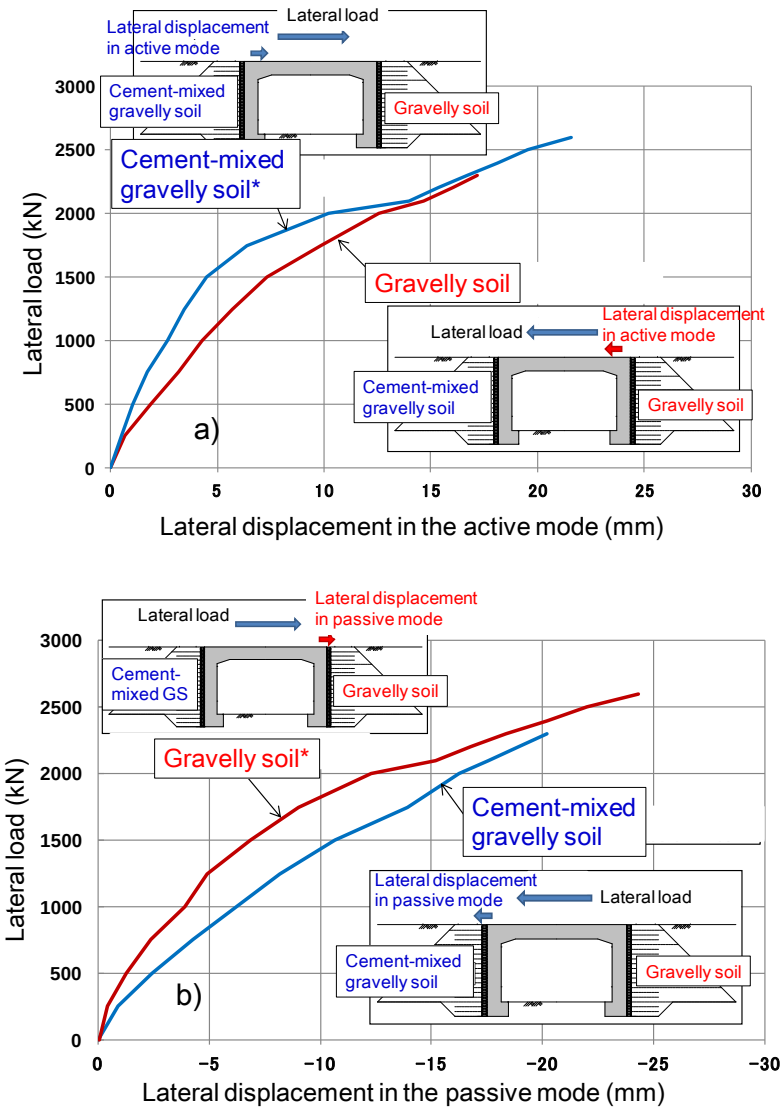

Figure 12. Envelopes of the relationships between the lateral load and the lateral displacements at the top of the facings for displacements in: a) active mode; and b) passive mode, from reversed lateral cyclic loading tests.

Fig. 13 shows the time histories of the increase in the tensile strain due to reversed cyclic loading. It may be seen that, at two points from the back face of the facing for the cement-mixed GS approach block, the increase in the geogrid tensile strains was very large and substantially larger than the one in the gravelly soil approach block. In the last cycle, the tensile force in the geogrid inside the gravel bag zone between the facing and the cement-mixed GS exceeded the rupture strength. Yet, this trend of behavior did not result in a sudden increase in the displacement in the active mode at the top of the facing for the cement-mixed GS backfill in the last cycle of loading (Figs. 11a & 12a).

The trend of behaviour explained above means that the coefficient of geogrid stiffness, K_s, at the back of the facing for the cement-mixed GS approach block is significantly higher than the value for the gravelly soil approach block. This trend

is due likely to that the deformation of geogrid in the cement-mixed GS backfill is much more strongly restrained than the one in the gravelly soil backfill. This point can also be confirmed by the fact that the geogrid strain at a distance of 150 cm back from the facing is nearly zero in the cement-mixed GS backfill, while it is noticeable in the gravelly soil backfill.

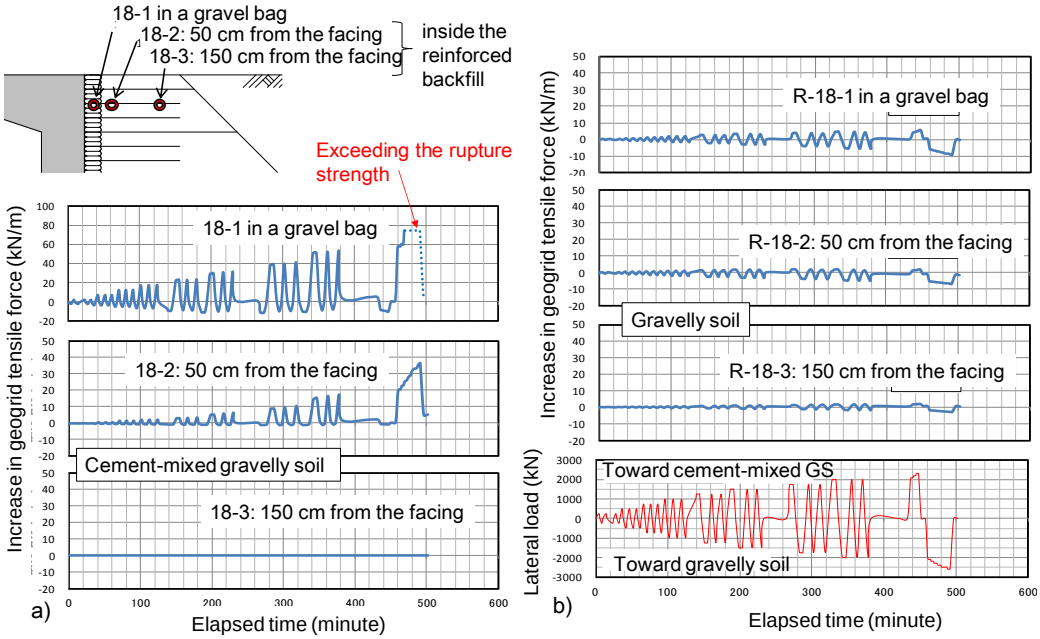

Figure 13. Time histories of earth pressure near the top of the facing in the reversed cyclic loading test in the approach blocks of: a) cement-mixed gravelly soil; and b) gravelly soil.

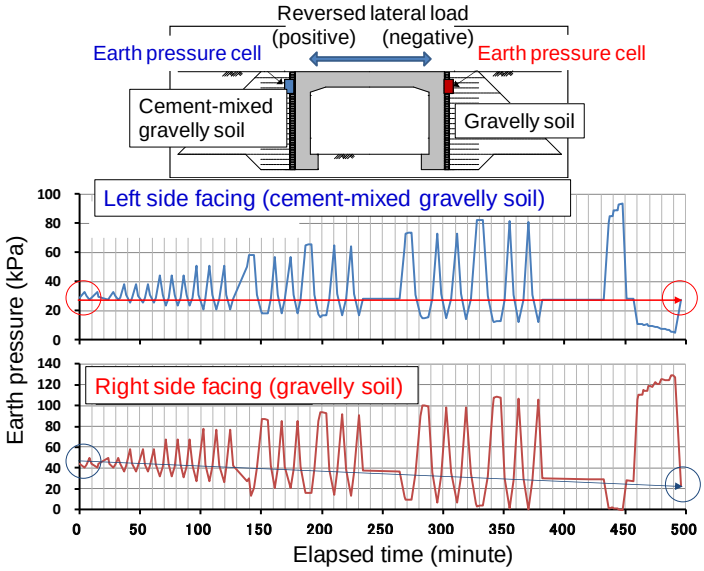

Figure 14. Time histories of earth pressure near the top of the facing in the reversed cyclic loading test

Fig. 14 shows the time histories of earth pressure near the top of the facings for

the two approach blocks of cement-mixed GS and gravelly soil. It may be seen that the increase in the passive earth pressure was much larger than the decrease in the active earth pressure, showing that the approach blocks resisted the lateral load mainly by developments of large passive pressure. It may also be seen that the peak passive earth pressure on the facing of the gravelly soil approach block became gradually larger than the one on the facing of the cement-mixed GS approach block. This may be due to that the ratchet mechanism [1] was more significant in the gravelly soil approach block. That is, the active displacement of the active zone in the backfill (which is the gravel bag zone and the gravelly soil approach block) that develops when subjected to active displacement of the facing was not recovered when the facing subsequently displaces in the passive mode. Therefore, the residual vertical downward displacement of the active zone accumulates during cyclic loading, which results in a gradual increase in the passive earth pressure with cyclic loading. This trend was weaker in the cement-mixed GS approach block soil due to a high stability of the cement-mixed GS backfill.

After the lateral load exceeded about 1,500 kN, tensile cracks developed on the crests of both approach fills, corresponding to an increase in the facing displacements (Figs. 11 &12). Fig. 15a shows the crest of the cement-mixed GS approach block. It may be seen that the deformation in the approach block was concentrated to the boundary between the cement-mixed GS zone and the gravel bag zone. The development of this tension crack is likely associated with the event that the geogrid tensile force in the cement-mixed GS zone exceeded its tensile rupture strength (Fig. 13a). Yet, the crack width is very small, which does not become a problem for train running.

On the other hand, as seen from Fig. 15b, a tensile crack developed at the boundary between the gravelly soil zone and the gravel bag zone only when the facing displaced in the active zone and it disappeared upon unloading. A noticeable tensile crack with a width of about 10 mm developed at a distance of 3.9 m back from the facing (outside the approach block). These trends of behavior indicate that the facing displacement reached deeper zones in the gravelly soil approach block than in the cement-mixed GS approach block, as seen from the development pattern of geogrid strain (Fig. 13).

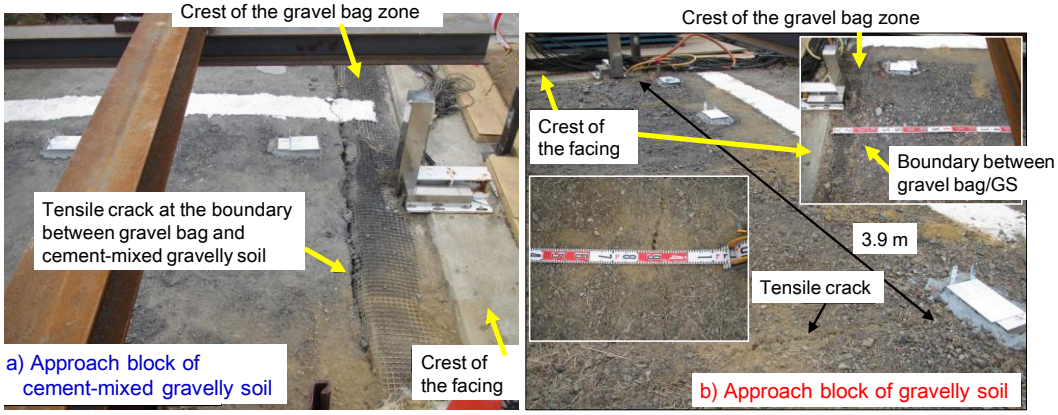

Figure 15. Deformation of the crest of the approach block of: a) cement-mixed GS; and b) gravelly soil, seen after reversed lateral cyclic loading tests

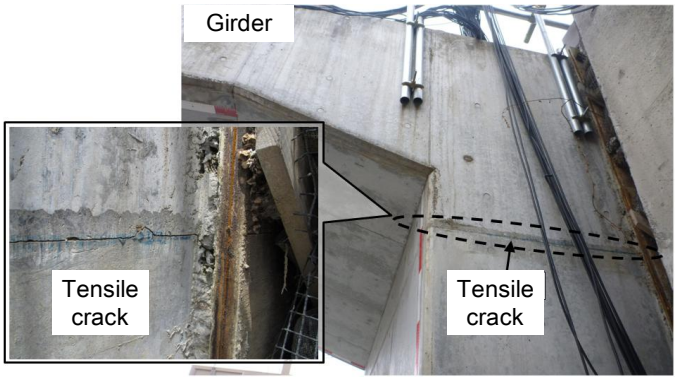

Figure 16. Tensile crack in the facing for the cement-mixed GS approach block that developed when the facing displaced in the active mode by lateral load of 2,600 kN.

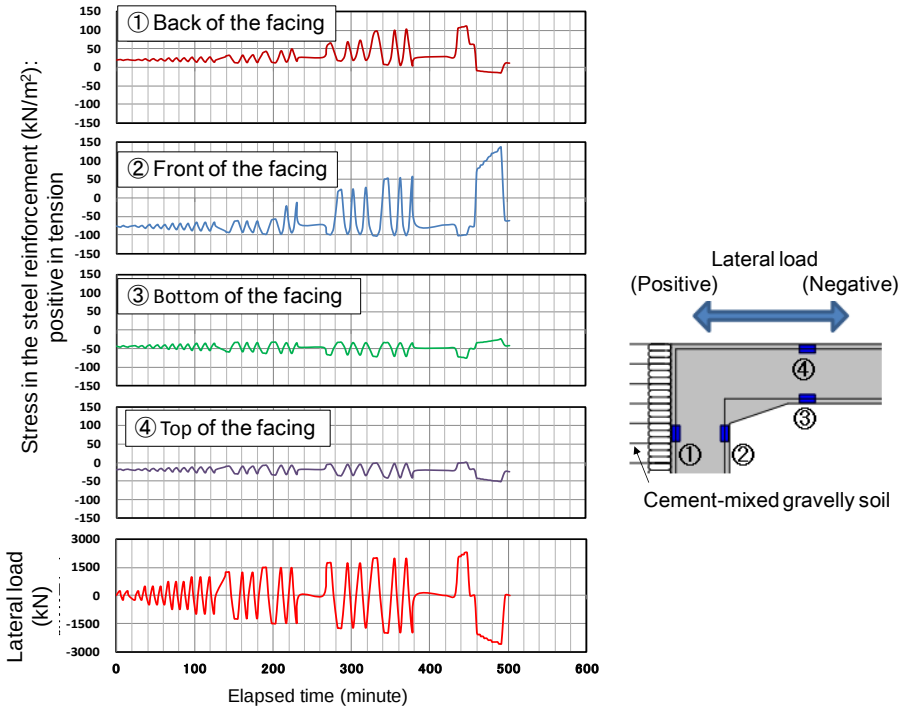

Figure 17. Time histories of steel strain around the girder/facing connection on the cement-mixed GS approach block side during the reversed cyclic loading test.

When the lateral load toward the gravelly soil approach block exceeded 2,300 kN, a horizontal tensile crack with a maximum width of 0.9 mm developed at the top construction joint in the facing for the cement-mixed GS approach block (Fig. 16). The structural damage by the development of this tensile crack is considered to be insignificant for the following reasons. Fig. 17 shows the time histories of steel strain around the girder/facing corner on the cement-mixed GS approach block side during the reversed cyclic loading test. The largest tensile strain, equal to 150 kN/mm^2, developed at point 2 (on the front side of the facing immediately below the hunch at the girder/facing connection) when the facing displaced in the active mode by the peak lateral load of 2,600 kN (exceeding the Level 2 seismic load). This behaviour is consistent with the development of a tensile crack seen in Fig. 16. Yet, the largest steel tensile force in this test, 150 kN/mm^2, is still substantially

lower than the yield stress for SD345, equal to 345 N/mm^2. These observations indicate that this GRS integral bridge model exhibits no serious structural damage even by Level 2 seismic load.

CONCLUSIONS

The following conclusions can be derived from the results from two types of lateral cyclic loading tests on a full-scale model of GRS integral bridge described above:

1) *One-side cyclic loading tests simulating thermal effects by a temperature change of 20^o in centigrade for a girder length of 14.75 m*: no significant increase took place in the earth pressure on the back of the facing and the settlement of the backfill was negligible. These results show that, at least within the limit of the conditions in these tests, the thermal effects are negligible.
2) *Reversed cyclic loading tests simulating seismic loading reaching L2 design seismic load*: When the lateral load equivalent to the inertia of the girder by L2 seismic load was fully applied to the abutments of the GRS integral bridge model, some noticeable effects were observed: i.e., the tensile force in the geogrid at some places reached its rupture strength, thin tensile cracks developed on the crest of the approach blocks and a horizontal tensile crack developed at the construction joint of the facing. However, the damage level is substantially below the level at which repair works become necessary, showing that the GRS integral bridge has a very high seismic stability.

ACKNOWLEDGEMENTS

This study was financially supported by the Ministry of Land, Infrastructure, Transport and Tourism.

REFERENCES

1. Tatsuoka, F., Hirakawa, D., Nojiri, M., Aizawa, H., Nishikiori, H., Soma, R., Tateyama, M. and Watanabe, K. 2009. "A new type integral bridge comprising geosynthetic-reinforced soil walls", *Gesynthtetics International, IS Kyushu 2007 Special Issue*, 16(4): pp.301-326.
2. Tatsuoka, F., Hirakawa, D., Nojiri, M., Aizawa, H., Nishikiori, H., Soma, R., Tateyama, M. and Watanabe, K. 2010. "Closure to Discussion on "A new type of integral bridge comprising geosynthetic-reinforced soil walls", *Gesynthtetics International*, **17**, No.4, pp.1-12.
3. Tatsuoka, F. 1992. "Roles of facing rigidity in soil reinforcing", *Keynote Lecture, Proc. Earth Reinforcement Practice, IS-Kyushu '92* (Ochiai et al. eds.), Vol.2: pp.831-870.
4. Tatsuoka, F., Tateyama, M, Uchimura, T. and Koseki, J. 1997. "Geosynthetic-reinforced soil retaining walls as important permanent structures", *Mercer Lecture, Geosynthetic International*, Vol.4, No.2, pp.81-136.
5. Yonezawa, T., Yamazaki, T., Tateyama, M. and Tatsuoka, F. 2013. "Various geosynthetic-reinforced soil structures for Hokkaido high-speed train line", *Proc. International Symposium on Design and Practice of Geosynthetic-Reinforced Soil Structures, Oct. 2013, Bologna* (Ling et al., eds.) (to appear).
6. Tatsuoka, F., Tateyama, M. and Koseki, J. 2012. "GRS structures recently developed and constructed for railways and roads in Japan", Keynote lecture, *Proc. 2nd International Conference on Transportation Geotechnics (IS-Hokkaido 2012)* (Miura et al., eds.), pp.63-84.

7. Tatsuoka, F., Tateyama, M., Koseki, J. and Yonezawa, T. 2013. “Geosynthetic-reinforced soil structures for railways twenty five year experiences in Japan”, *Geotechnical Engineering Journal of the SEAGS & AGSSEA* (to appear).

8. Nagatani, T., Tamura, Y., Iijima, M., Tateyama, M., Kojima, K. and Watanabe, K. 2009. “Construction and field observation of the full-scale test integral bridge”, *Geosynthetics Engineering Journal*, Vol.24, pp.219-226.

9. Tatsuoka,F., Tateyama,M., Murata,O. and Tamura,Y. 1994. “Geosynthetic-reinforced soil retaining wall structures with short reinforcement and a rigid facing (closure)”, *Proc. of Int. Symposium Recent Case Histories of Permanent Geosynthetic-Reinforced Soil Retaining Walls* (Tatsuoka and Leshchinsky eds.), Balkema, pp.323-342.

10. Yazaki, S., Tatsuoka, F., Tateyama, M., Koda, M., Watanabe, K. and Duttine, A. 2013. “Seismic design of GRS integral bridge”, *Proc. International Symposium on Design and Practice of Geosynthetic-Reinforced Soil Structures, Oct. 2013, Bologna* (Ling et al., eds.) (to appear).